Effect of packaging pressure on energy harvesting from vibration source

Tianyang Wang[1], Yulong Zhang[1,2], Xingwei Chen[1], Anxin luo[1] and Fei Wang[1,2]

[1] Dept. Electrical and Electronic Engineering, Southern University of Science and Technology, Shenzhen 518055, China
[2] Shenzhen Key Laboratory of 3rd Generation Semiconductor Devices, Shenzhen 518055, China

E-mail: wangf@sustc.edu.cn, wangty@mail.sustc.edu.cn

Abstract. In this paper, we have studied the effect of air pressure damping on the vibration-based energy harvesting devices. The device we used is an electrostatic energy harvester with an out-of-the-plane gap closing scheme. A broadened bandwidth is observed at 4 Pa when the acceleration is increased from 0.5 m/s^2. A power output of 2.2 μW is achieved at the air pressure of 4 Pa when a low acceleration of 0.5 m/s^2 is applied, while the power output is only 0.02 μW at atmosphere with an acceleration of 1.2 m/s^2. Detailed study is made to investigate the waveform of the displacement and the voltage output. Nonlinearity is observed at low air gas pressure about 239 Pa and it is more significant at 4 Pa.

1. Introduction

Recently, energy harvesters has been developed a lot because of the incomparable highlights as an alternative choice to replace the button cells in the wireless sensor networks, micro systems and in-body health monitoring devices [1-2]. Among various energy harvesters, the vibration-based energy harvesting devices (VEHD) use the vibration-to-electricity conversion methods to convert kinetic energy to electric energy. VEHD based on the piezoelectric [3-6], electromagnetic [7-9] and electrostatic methods [10-17] have been developed during the past years. For most of the VEHD, the performance of the devices has been generally studied with a few governing equations [18]. However, there is not much attention has been paid for the damping force in the energy harvesters. In this paper, we will study how the air pressure affects the performance of VEHD.

To evaluate the air pressure effect, we have designed an electrostatic VEHD with an out-of-the-plane gap closing scheme, as shown in Figure 1. The device can be simply regarded as a variable capacitor with parallel electrodes on two separate plates as shown in Figure 2. When the proof mass is driven by an ambient vibration source, induced charge caused by the pre-charged CYTOP electret moves back and forth between the two electrodes, which generates a current through an external load. The overall size of the device we used is about 13×18 mm^2, and the surface potential of the electret is charged to about -400 V. During the vibration, the squeeze air damping force would affect the mechanical performance of the proof mass and therefore influence the output power.

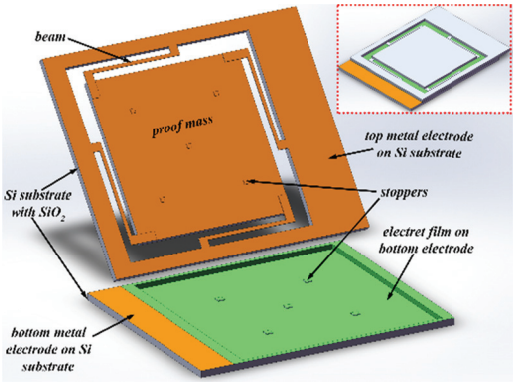

Figure 1. 3D schematic of the out-of-plane electrostatic energy harvesting device.

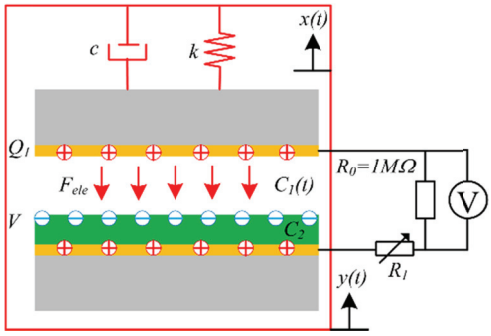

Figure 2. Schematic of the energy transduction between the mechanical system and the electric circuit with external

2. Characterization

The effect of air pressure on the performance of the VEHD is characterized with the equipment setup shown in Figure 3. It consists of a chamber where the pressure can be controlled with a pump and monitored with a pressure sensor. A shaker is put in the chamber to mimic the vibration source as described in [19]. A laser detector is used to monitor the displacement of the proof mass during the vibration. By tuning the air pressure, we can characterize the device performance under various damping conditions.

The performance test circuit is shown in Figure 2. The output power can be calculated by measuring the voltage across a fixed resistance R_0=*1 MΩ* while the overall optimal load resistance is *17 MΩ*. The whole experiment to characterize the air pressure effect of VEHD can be divided into two parts to achieve convincing results.

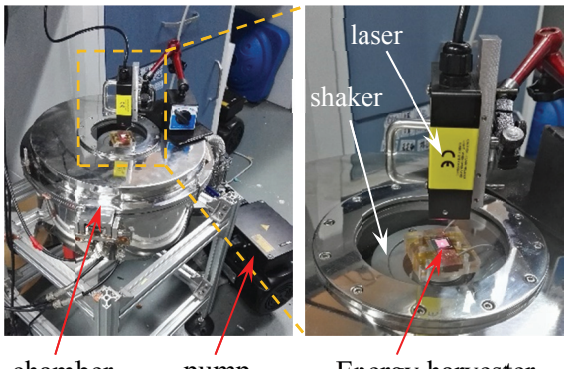

Figure 3. The measurement setup for the air damping effect.

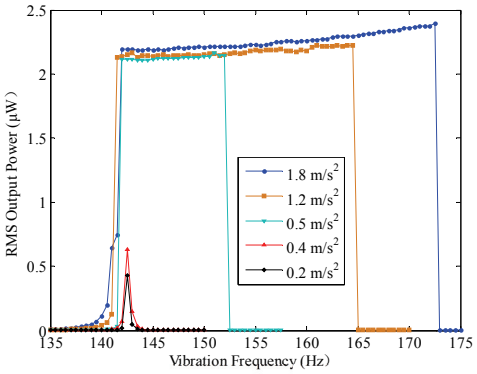

Figure 4. The relationship between the vibration frequency and the output power of the energy harvester at a low air pressure of

2.1. Bandwidth at low air pressure

This part of the experiment starts with pumping down the ambient gas pressure in the chamber. Then a sinusoidal signal is given from the signal generator (Brüel&Kjær, LAN-XI 3160) and a power amplifier (Brüel&Kjær, 2719) to excite the shaker and the device.

The result is shown in Figure 4. Five different accelerations are applied on the VEHD at a low air pressure of 4 Pa. It is clear that a maximal power of 2.2 μW is achieved at low acceleration of 0.5 m/s^2 and a bandwidth is continuously broadened when the vibration amplitude is increased from 0.5 m/s^2 to 1.8 m/s^2, which could be interesting for energy harvesting from random vibration sources. A broad

bandwidth of about 30 Hz (from 142 Hz to 172 Hz) has been observed at an acceleration of 1.8 m/s^2. This is because large vibration amplitude could be easily reached when low air pressure is applied in the chamber. As it is shown in Figure 7(a), a maximum displace of the proof mass is measured up to 250 μm, which is exactly the gap between the stoppers of the two plates.

2.2. Output power with changing air pressure

The energy loss caused by air pressure damping can be clearly seen in this part. When the chamber pressure is increased, higher vibration amplitude is needed to achieve the same power, as shown in Figure 5.

The air damping effect can be more clearly seen in Figure 6. With a fixed vibration amplitude of 1.2 m/s^2, the RMS power of the device at resonance decreases gradually from 2.2 μW to about 0.02 μW when the chamber pressure increases from 4 Pa to atmosphere.

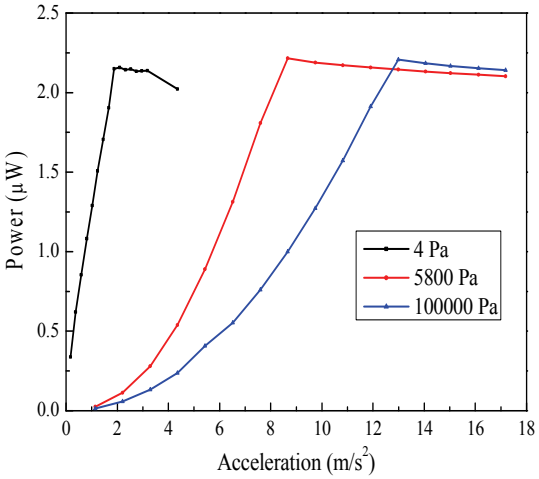

Figure 5. The output power of the energy harvester with increased acceleration amplitude under different air pressure of 4 Pa, 5800 Pa and 10^5 Pa, respectively.

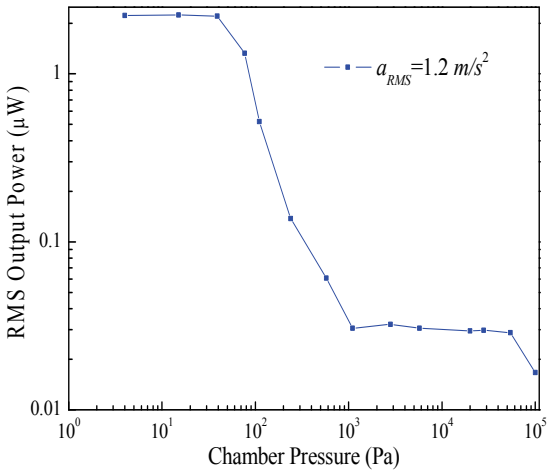

Figure 6. The output power of the energy harvester at resonance with chamber pressure increased from 4 Pa to atmosphere.

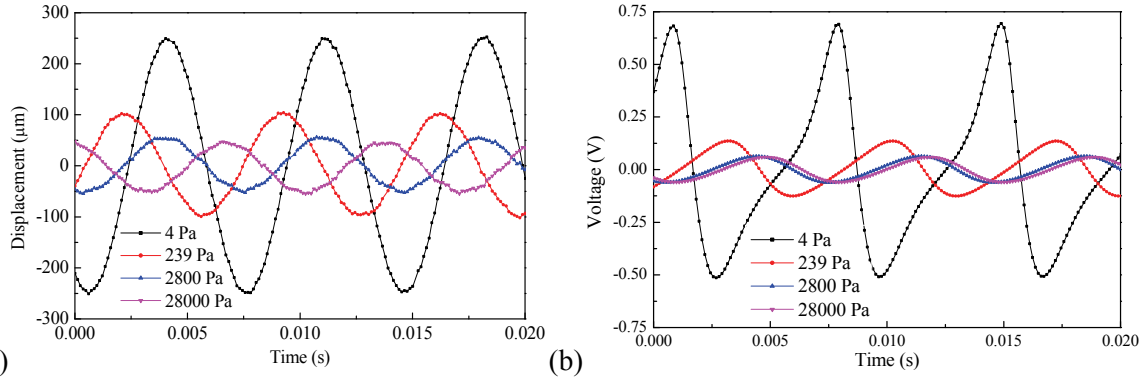

(a) (b)

Figure 7. (a) The displacement of the proof mass and (b) the waveform of the voltage output on R_0 at the same vibration amplitude of 1.2 m/s^2 when the chamber pressure is tuned to 4 Pa, 239 Pa, 2800 Pa and 28000 Pa, respectively.

A more detailed study has been done to investigate the waveform of the displacement and the voltage output when the chamber pressure is increased, as shown in Figure 7. The displacement amplitude of the proof mass decreases/stabilizes to 55 μm under a chamber pressure of 2800 Pa, and the voltage output amplitude increases from 0.1 V to 0.65 V. Nonlinearity can be observed at the ambient gas pressure of 239 Pa, and it is more obvious at 4 Pa. The nonlinearity effect is mainly due to

the fact that the capacitance between the two electrodes is inversely proportional to gap distance [16]. Furthermore, when the two plates of device get close enough, the electrostatic force will influence the output voltage.

3. Conclusion

A primary research was made to find the effect of air pressure damping on VEHD. A broadened bandwidth can be observed when the acceleration is increased from 0.5 m/s^2. At a low air pressure of 4 Pa, maximum power output of 2.2 μW can be achieved with a low acceleration of 0.5 m/s^2. When the air pressure increases up to atmosphere, the power output drops down to 0.02 μW. When the ambient gas pressure is low enough, the waveform of the voltage output will become nonlinear for the variation of the capacitance.

Acknowledgement

This work is supported by National Natural Science Foundation of China (Project No.: 51505209) and University Research Committee of SUSTech (Project No.: FRG-SUSTC1501A-31). Fei Wang is also supported by Guangdong Natural Science Funds for Distinguished Young Scholar (Project No.: 2016A030306042).

References

[1] S. P. Beeby, M. J. Tudor, and N. M. White, Meas. Sci. Technol., 17 (2006), pp. R175-R195.
[2] P. D. Mitcheson, E. M. Yeatman, G. K. Rao, A. S. Holmes, and T. C. Green, P. IEEE, 96 (2008), pp. 1457-1486.
[3] L. Tang and Y. Yang, Appl. Phys. Lett., 101 (2012), 094102.
[4] S. Li, Z., A. Zhang, and F. Wang, AIP Adv., 6 (2016), pp.015019.
[5] Q. Shi, T. Wang and C. Lee, Sci. Rep., 6 (2016), pp. 24946.
[6] Q. C. Tang and X. X. Li, IEEE/ASME Trans. Mech., vol. PP, no. 99, pp. 1-7, Jan. 2014.
[7] S. P. Beeby, et.al., J. Micromech. Microeng., 17 (2007), pp. 1257–1265.
[8] M. Wischke, M. Masur, F. Goldschmidtboeing, and P. Woias, J. Micromech. Microeng.,, Volume 20, Number 3, 035025 (2010).
[9] I. Sari, T. Balkan, and H. Kulah, Sensor Actuat. A-Phys, 145–146(2008), 405.
[10] T. Takahashi, M. Suzuki, T. Nishida, Y. Yoshikawa, and S. Aoyagi, in Proc. MEMS 2015, pp. 1145–1148, 2015.
[11] T. Tsutsumino, Y. Suzuki, N. Kasagi, and Y. Sakane, Proc. MEMS 2006, pp. 98–101, 2006.
[12] Y. Xu, et.al., Micro & Nano Letters, 2016, DOI: 10.1049/mnl.2016.0336.
[13] F. Wang, C. Bertelsen, G. Skands, T. Pedersen, and O. Hansen, Microelectronics Engineering, 97 (2012), pp. 227–230.
[14] A. Crovetto, F. Wang, and O. Hansen, J. Micromech. Microeng., 23 (2013), 114010 (10pp).
[15] F. Wang, and O. Hansen, Sensor Actuat. A-Phys, 211 (2014), pp.131–137.
[16] S. Boisseau, G. Despesse, T. Ricart, E. Defay, and A. Sylvestre, Smart Mater. Struct., 20 (2011), p. 105013.
[17] Y. Suzuki, IEEJ T. Electr. Electr., 6 (2011), pp. 101–111.
[18] A. Crovetto, F. Wang, and O. Hansen, J. Microelectromechan. Sys., 23 (2014), pp. 1141-1155.
[19] S. Li, et.al., Sensor Actuat. A-Phys, 247 (2016), pp. 547–554.